MNRAS **000**, 1–5 (2017) Preprint 23 March 2017 Compiled using MNRAS LATEX style file v3.0

The dust-to-ices ratio in comets and Kuiper belt objects

Marco Fulle,[1⋆] V. Della Corte,[2] A. Rotundi,[2,3] S. F. Green,[4] M. Accolla,[5] L. Colangeli,[6] M. Ferrari,[2] S. Ivanovski,[2] R. Sordini,[2] and V. Zakharov[7,8]
[1] *INAF - Osservatorio Astronomico, Via Tiepolo 11, I-34143 Trieste, Italy*
[2] *INAF - Istituto di Astrofisica e Planetologia Spaziali, Via Fosso del Cavaliere 100, 00133 Rome, Italy*
[3] *Universitá degli Studi di Napoli Parthenope, Dip. di Scienze e Tecnologie, CDN IC4, 80143 Naples, Italy*
[4] *Planetary and Space Sciences, School of Physical Sciences, The Open University, Milton Keynes MK7 6AA, UK*
[5] *INAF - Osservatorio Astronomico di Catania, via S. Sofia 78, 95123 Catania, Italy*
[6] *ESA - ESTEC, European Space Agency, Keplerlaan 1, 2201 AZ Noordwijk, The Netherlands*
[7] *LESIA-Observatoire de Paris, CNRS, UPMC, Universite Paris-Diderot, 5 place Jules Janssen, 92195 Meudon, France*
[8] *Sorbonne Universites, UPMC Univ Paris 06, CNRS, Laboratoire de Meteorologie Dynamique, 4 place Jussieu, 75252, Paris, France*

Accepted XXX. Received YYY; in original form ZZZ

ABSTRACT
Comet 67P/Churyumov-Gerasimenko (67P hereinafter) is characterised by a dust transfer from the southern hemi-nucleus to the night-side northern dust deposits, which constrains the dust-to-ices mass ratio inside the nucleus to values a factor two larger than that provided by the lost mass of gas and non-volatiles. This applies to all comets, because the gas density in all night comae cannot prevent the dust fall-back. Taking into account GIADA data collected during the entire Rosetta mission, we update the average dust bulk density to $\rho_D = 785^{+520}_{-115}$ kg m^{-3} that, coupled to the 67P nucleus bulk density, confirms an average dust-to-ices mass ratio $\delta = 7.5$ inside 67P. The improved dust densities are consistent with a mixture of $(20 \pm 8)\%$ of ices, $(4 \pm 1)\%$ of Fe-sulphides, $(22 \pm 2)\%$ of silicates, and $(54 \pm 5)\%$ of hydrocarbons, on average volume abundances. These values correspond to solar chemical abundances, as suggested by the elemental C/Fe ratio observed in 67P. The ice content in 67P matches that inferred in Kuiper Belt Objects (KBOs hereinafter), $(20 \pm 12)\%$ on average volume abundance, and suggests a water content in all Trans-Neptunian Objects (TNOs hereinafter) lower than in CI-chondrites. The 67P icy pebbles and the dust collected by GIADA have a microporosity of $(49 \pm 5)\%$ and $(59 \pm 8)\%$.

Key words: comets: general – comets: individual: 67P/Churyumov–Gerasimenko – Kuiper belt: general – Kuiper belt objects: individual: Pluto, Charon, Triton – protoplanetary discs – space vehicles

1 INTRODUCTION

While ground-based coma observations provide reliable measurements of the water loss rate, unrealistic assumptions of the dust size distribution have often provided strong underestimates of the dust loss rate from comets (Newburn & Spinrad 1985), with the consequence that the dust-to-ices mass ratio δ has been often assumed < 1. **Here with dust we refer to the total non-volatile component of a comet nucleus. Often, the dust size distribution was assumed very steep, with both the dust mass and optical brightness dependent on micron-sized particles, opposite to what has been observed with Rosetta, with the 67P dust mass dependent on the largest ejected chunks, and the optical brightness on mm-sized particles (Rotundi et al. 2015; Fulle et al. 2016a).** For example, Kresak & Kresakova (1987) provided the loss rates from most Jupiter Family Comets (JFCs hereinafter) assuming $\delta = 1/3$. In 67P, Kresak & Kresakova (1987) estimated a water loss rate per orbit about 20% larger than actual measurements (Bertaux 2015; Shinnaka et al. 2017). The Giotto mission to comet 1P/Halley showed that $\delta > 1$ and a more recent analysis of the Giotto dust data provided $3 < \delta < 40$ (Fulle et al. 2000). This result confirmed the δ estimates for JFCs (Sykes & Walker 1992a) based on the first ground-based observations able to infer reliable dust mass loss rates, derived by models of the IRAS dust trails (Sykes & Walker 1992b). Regarding 67P, Sykes & Walker (1992a) found $\delta = 4.6$, a good prediction of the values later confirmed by the Rosetta mission in the material lost by the comet, $\delta = 4 \pm 2$

⋆ E-mail: fulle@oats.inaf.it (MF)

(Rotundi et al. 2015). In the same paper, Sykes & Walker (1992a) **showed that the low bulk density of Pluto and Triton is consistent with the same volume abundances of dust and ices (of bulk density of 3000 and 1000 kg m^{-3}, respectively) in these bodies. This implies $\delta \approx 3$ and a common origin of all TNOs**. This approach neglects the presence of hydrocarbons in the non-volatile mass of TNOs, although the CHON particles observed in 1P/Halley are mostly hydrocarbons (Jessberger et al. 1989). Best terrestrial analogues of hydrocarbons in the protoplanetary disc are soft hydrogenated carbon alloys (Robertson 2002), with a bulk density close to that of ices and a hardness up to 10 GPa, a factor ten larger than the central pressure of Pluto and Triton. The bulk density of TNOs may be due either to abundant ices or to hydrocarbons (Fulle 2017). Models of Pluto and Charon assume a hydrocarbons-to-silicates mass ratio $h/s = 0.2$, which implies $\delta = 1.5$ (McKinnon et al. 1997). In 1P/Halley, the elemental abundances provide $h/s > 0.9$ and a ratio C/Mg = 8 (Jessberger et al. 1989), which is larger than the solar ratio C/Mg = 7 (Lodders 2003) and cannot constrain δ. All these facts indicate that we cannot infer the real structure of comets and KBOs without fixing the ratios δ and h/s (Fulle 2017), which is the aim of this paper.

2 67P DUST DEPOSITS PROVIDE δ

The Rosetta mission has observed dust deposits many metres thick and mostly composed of particles of mass > 1 mg (Fulle et al. 2016b), which cover about 80% of the 67P northern hemi-nucleus (Keller et al. 2015b). The coherent orientation of tail-like features around boulders embedded in the dust deposits indicates a dust flow from south to north (Mottola et al. 2015). This implies that the deposits are built-up by a dust transfer occurring mainly at perihelion, when the comet activity is at its maximum, and most of the southern hemi-nucleus is in a seasonal polar summer and eroded of many metres (Keller et al. 2015b). At the same time, most northern hemi-nucleus is in a seasonal polar night: the very low gas pressure above that surface (and possibly the recondensation of some water from the coma back to the surface) makes the deposition on the night-side nucleus surface most efficient (Fulle et al. 2016b). **67P currently has a very stable spin axis orientation (Jorda et al. 2016), with consequent stable seasons and a northern polar night lasting all the perihelion phase. A stable spin axis is a necessary condition to cumulate thick deposits on the northern hemi-nucleus. On the contrary, the process of dust transfer from the sunlit nucleus surface to the night-side one is independent of the duration of the polar night, because the physics of the night coma is independent of the spin stability. The day-to-night dust transfer is probably very similar in all comets, because the nucleus surface temperature on the night side, and therefore the gas outflow, is similarly low in all comets. Thus, the cut-off dust mass, below which the fall-back on the nucleus becomes less and less efficient, depends mainly on the nucleus mass. In 67P, the dust fall-back is efficient at masses > 1 mg (Fulle et al. 2016b). This cut-off dust mass becomes even lower for comet nuclei of mass larger than that of 67P, and larger for the few comets with a lighter nucleus, e.g. 103P/Hartley 2. In this comet, dust deposits are further thinned by its unstable spin, with a fast and large precession excited by the gas torque on the light nucleus, so that the day-to-night dust transfer has no time to build-up thick deposits, which are eroded once the night surface is exposed to the sun.**

The 67P dust deposits offer us a unique opportunity to measure the dust mass involved in the day-to-night dust transfer. **The dust in the coma and the deposits have the same water mass fraction Z, because the sublimation lifetime of dust is much longer than the day-to-night dust transfer, as shown below. The water mass fraction $X \approx 6\%$ which is sublimating from the nucleus surface has been evaluated by thermo-physical models of the nucleus surface (Keller et al. 2015b; Blum et al. 2017). It** is linked to the water mass fraction Y of the pristine terrains and to Z by means of two equations for the northern and the southern hemi-nuclei, respectively

$$(1-b)\ Y + b\ Z = aX \tag{1}$$

$$X + Z = Y \tag{2}$$

where Y provides the dust-to-water mass fraction $\delta_{water} = Y^{-1} - 1$ inside the nucleus, $b \approx 0.8$ **is the fraction of the northern nucleus surface covered by dust deposits (Keller et al. 2015b)** and $a \approx 1.05$ **takes into account an active spot in Hapi (Fulle et al. 2016b), with an area about 1/20 of the northern hemi-nucleus and with X a factor about ten larger than the average on the nucleus surface (Fougere et al. 2016).** Eq. (2) describes a pristine surface exposed by the erosion of many metres (Keller et al. 2015b), with a water mass fraction Y partly released by water sublimation (X) and partly trapped in the ejected dust (Z). **Eqs. (1) and (2) provide $Y = (a+b)\ X \approx 11\%$, $Z = (a+b-1)\ X \approx 5\%$ and $\delta_{water} \approx 8$, which is larger than $\delta_{water} \approx 5$ provided by the dust and gas loss rates from 2 au to perihelion (Fulle et al. 2016a). 3D coma models constrain the gas loss rate from the coma dust to a fraction $c < 5\%$ of that coming from the nucleus (Fulle et al. 2016b), so that the dust particles in the coma release a water loss rate $c\ Q_w$ from their total water mass $Z\ M_d$, where $Q_w = 400 \pm 50$ kg s^{-1} is the 67P perihelion water loss rate (Shinnaka et al. 2017) and $M_d \approx 3\ 10^8$ kg is the dust mass in particles of mass > 1 mg. M_d has been computed inside the Rosetta orbit of radius $R \approx 400$ km, where the mass in dust particles is $R\ Q_m/v$ in the case of a spherical expansion at constant speed v. The mass loss rate Q_m and v are provided by OSIRIS data (Fulle et al. 2016a). Actually, the mass in particles is larger, due to the dust acceleration from the nucleus surface to the distance R. Particles reaching a nucleus distance larger than R have a negligible probability to fall back into the deposits. The day-to-night transfer lasts much less than $Z\ M_d/(c\ Q_w) > 8$ days on average, supporting the assumption of the same Z in the dust deposits and in the coma dust.**

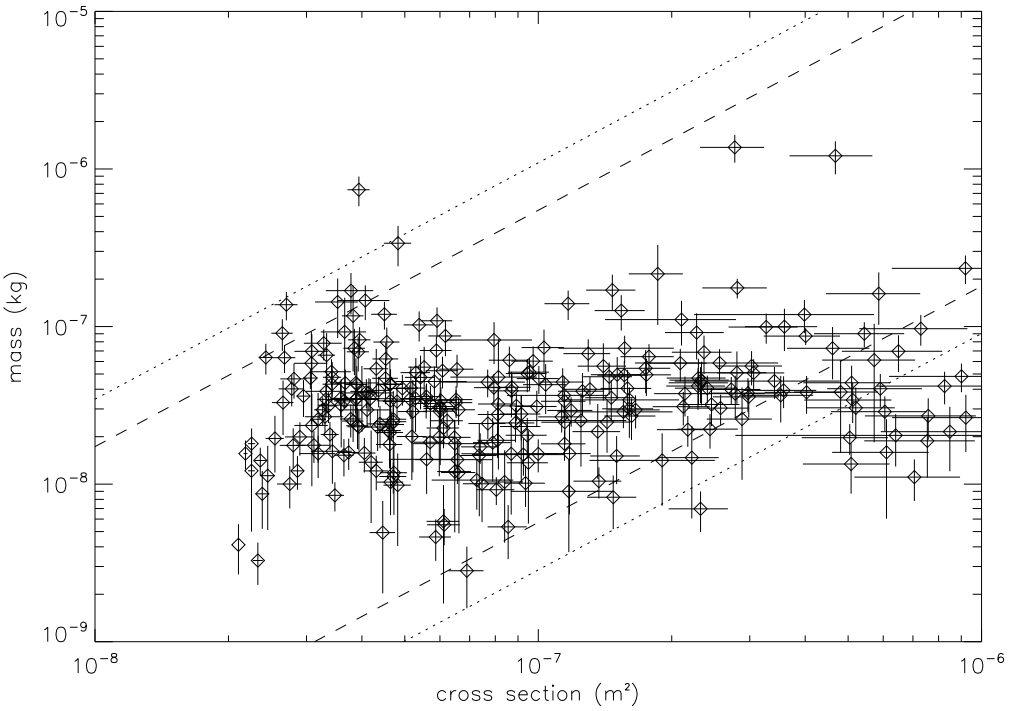

Figure 1. Mass and cross-section χ measurements of compact particles detected by GIADA from August 2014 to September 2016 (the error bars refer to $1-\sigma$ standard error of the 271 GDS+IS measurements). The data are compared with the trends of prolate and oblate ellipsoids of aspect ratio of ten (dotted lines) and five (dashed lines) and with dust bulk densities of Fe-sulfides, $\rho_1 = 4600$ kg m^{-3} (upper lines), and of hydrocarbons, $\rho_3 = 1200$ kg m^{-3} (lower lines). Particles located below the lower lines have a high porosity. The GDS signal saturates at $\chi > 10^{-6}$ m^2. Particles with $\chi < 2 \times 10^{-8}$ m^2 (and most of those with mass $< 10^{-8}$ kg) were too small and fast to be detected by GDS. The flux at masses $> 2 \times 10^{-7}$ kg was very low during the entire mission due to the spacecraft safety constraints.

RSI (Radio Science Investigation) onboard Rosetta measured a total mass loss from 67P nucleus of $(1.1\pm0.3)\ 10^{10}$ **kg from 2014, August, to 2016, September (Pätzold et al. 2016). During the same period, Hansen et al. (2016) estimated a water loss of** $6.4\ 10^9$ **kg by modeling Rosetta in-situ data, with a maximum water loss rate of** $(3.5\pm0.5)\ 10^{28}$ **mol s^{-1}, a factor 3 larger than provided by Earth-orbiting satellites,** $(1.3 \pm 0.15)\ 10^{28}$ **mol s^{-1} (Shinnaka et al. 2017). This is inconsistent with e.g. water distributed sources, which imply in-situ measurements of the water loss rate lower than Earth-based ones. Such a systematic error of the water loss rate estimated by Hansen et al. (2016) at perihelion is confirmed by the overestimate by a factor 4 of the IR water flux modeled by Hansen et al. (2016) and Fougere et al. (2016) with respect to that measured by VIRTIS (Visible and Infrared Thermal Imaging Spectrometer, Bockelée-Morvan et al. (2016)), which makes VIRTIS water data consistent with Earth-based ones (Bertaux 2015; Shinnaka et al. 2017) and with the water loss rate fitting the acceleration of the 67P nucleus spin (Keller et al. 2015a). Taking into account the systematic correction of the total water loss provided by Hansen et al. (2016), it becomes consistent with previous estimates of** $2.7\ 10^9$ **kg (Bertaux 2015; Keller et al. 2015b), so that the RSI measurements provide** $\delta_{water} = 3 \pm 1$**, again significantly lower than** $\delta_{water} \approx 8$ **provided by Eqs. (1) and (2).** This difference measures the dust mass involved in the day-to-night transfer. If δ_{water} inside the nucleus were exactly that inferred for the lost material, the dust mass deposited on the night side would be exactly zero, according to the assumption that all the dust is lost in space. Instead, to obtain dust deposits, δ_{water} inside the nucleus has to be significantly larger than the values observed in the lost material. **In 67P, if the lost material has** $\delta_{water} = 3$ **and the nucleus pristine material has** $\delta_{water} = 8$**, i.e. 16 dust unit masses and 2 water unit masses, then 1 water unit mass is lost in space and another remains on the surface, together with 13 dust unit masses, so that the dehydrated material remaining on the nucleus surface has a water mass fraction of 7%, in good agreement with the water mass fraction** $Z = 5\%$ **of the deposits.** We infer that probably in all comets δ_{water} inside the nucleus is about twice that measured in the lost material (e.g. by RSI or by means of JFC trail models).

3 GIADA DATA PROVIDE δ AND H/S

GIADA (Grain Impact Analyser and Dust Accumulator) onboard Rosetta measured the speed, the scattered light and the momentum of individual dust particles by means of two subsystems (Della Corte et al. 2014): a laser curtain plus photodiodes (GDS, Grain Detection System) and a plate

connected to piezoelectric sensors (IS, Impact Sensor). Here we consider the complete set of 271 coupled GDS+IS detections during the entire mission, from August 2014 to September 2016. Ongoing calibrations performed on the GIADA spare model with cometary dust analogues (Ferrari et al. 2014) allowed us to refine the mass and the geometrical cross section of the GDS+IS detections (Fig. 1) with respect to those reported in Fulle et al. (2016c). The new calibrations shifted four of the five data-points with bulk density > 4600 kg m^{-3} to the area between the dotted lines in Fig. 1, and increased the data uncertainty close to the saturation of the GDS signal. We follow here the procedure described by Fulle et al. (2016c) to compute the average dust bulk density in 67P by means of the dust masses and cross sections measured by GIADA (Della Corte et al. 2015), (Della Corte et al. 2016). The data in Fig. 1 provide the weighted average dust bulk density $\rho_D = 785^{+520}_{-115}$ kg m^{-3}, where the weights are the inverse of the bulk density error derived from each error pair in Fig. 1. ρ_D is linked to the non-volatiles-to-ices mass ratio inside the nucleus

$$\delta = \left[\frac{\rho_N}{\phi_G \ \rho_D} - 1 \right]^{-1} \tag{3}$$

where $\rho_N = 533$ kg m^{-3} is the 67P nucleus bulk density and $1 - \phi_G = 0.4$ is the nucleus macro-porosity (Fulle et al. 2016c). With $\rho_D = 785$ kg m^{-3}, we get $\delta = 7.5$ on average, consistent with $\delta_{water} \approx 8$ discussed in the previous section because at least 10% of 67P ices are composed of CO, CO_2 and O_2 (Fulle et al. 2016b). The lower and upper limits $\rho_D = 670$ kg m^{-3} and $\rho_D = 1300$ kg m^{-3} provide $\delta = 3.1$ and $\delta = \infty$, respectively. The 67P C/Fe ratio (Fray et al. 2016) is close to the solar end-case (Lodders 2003), so that the updated $\delta = 7.5$ and the solar elemental abundances constrain the free parameters of the structural equations of the 67P nucleus plotted in Figs. 2 and 3 of Fulle et al. (2016c), namely the micro-porosity and the volume abundances $c_1 = (4 \pm 1)\%$ of Fe-sulphides (bulk density $\rho_1 = 4600$ kg m^{-3}), $c_2 = (22 \pm 2)\%$ of silicates ($\rho_2 = 3200$ kg m^{-3} for Mg,Fe-olivines and pyroxenes, $\rho_2 = 2600$ kg m^{-3} for amorphous silicates (Fulle et al. 2016c)), and $c_3 = (54 \pm 5)\%$ of hydrocarbons ($\rho_3 = 1200$ kg m^{-3} (Robertson 2002)). The upper limits are obtained for compact ices and the lower limits for porous ices. The volume abundance of ices in 67P is $c_4 = (20 \pm 8)\%$, with the upper limit corresponding to porous ices. This value matches the volume abundances of ices found in ten parameter combinations valid for KBOs (between the end-cases of solar and CI-chondritic compositions), $c_4 = (20 \pm 12)\%$ (Fulle 2017). The updated micro-porosity of the pebbles, i.e. the icy building-blocks of the 67P nucleus, is $1 - \phi_P = (49 \pm 5)\%$. The dust micro-porosity is $1 - (1 - c_4)\ \phi_P = (59 \pm 8)\%$, where the factor $(1 - c_4)$ takes into account the voids left in the dust by the ices after sublimation. The bulk density of compacted dust becomes $\rho_D / [(1 - c_4)\ \phi_P] = 1925^{+2030}_{-560}$ kg m^{-3}. The upper limits of the micro-porosities and of the compacted bulk density are obtained for crystalline silicates and compact ices, the lower limits for amorphous silicates and porous ices.

4 DISCUSSION

Both 67P and KBOs contain only 1/5 of their volume as ice, thus less water than CI-chondrites (McKinnon et al. 1997). This suggests that bodies born close to the water snow-line contain more water than TNOs. This is consistent with the D/H ratios in 67P (Altwegg 2015) and 103P/Hartley 2 (Hartogh et al. 2011), which imply that 103P (apparently more water-rich than 67P) was born closer to the asteroidal belt than 67P (Fulle et al. 2016b). We have no data determining if the C/Fe ratio in 103P is lower than in 67P, i.e. closer to the CI-chondritic end-case, C/Fe < 1, than to the solar end-case, C/Fe $= 8.5$ (Lodders 2003). Although 1P/Halley shows a ratio C/Fe $= 16$ (Jessberger et al. 1989), even larger than the solar one, comets may also have a CI-chondritic C/Fe ratio, as it is confirmed by Stardust data and by KBOs. The composition of dust from comet 81P/Wild 2 is CI-chondritic, although the actual carbon bias on the data is unknown (Brownlee 2014). Fulle (2017) showed that Triton's bulk density is consistent with a CI-chondritic composition, not with a solar one. Fray et al. (2016) find that the 67P C/Fe ratio is close to the solar end-case, although the bias in the detections of 67P's C, Si and Fe remains unknown. In this case, the 67P ratios $h/s = (c_3\rho_3)/(c_2\rho_2)$, $c_2/c_1 = 5$, $c_3/c_1 = 12$ for porous ices and $c_3/c_1 = 14$ for compact ices match the values assumed to compute the KBO composition (Fulle 2017), and fix the largest possible KBO bulk density $c_5\rho_5$, where $c_5 = (1 + c_2/c_1 + c_3/c_1)^{-1}$ and $\rho_5 = \rho_1 + (c_2/c_1)\rho_2 + (c_3/c_1)\rho_3$ (Fulle 2017). Porous ices and crystalline silicates provide $h/s = 0.9$ and $c_5\rho_5 = 1944$ kg m^{-3}, which implies an ice surface layer on Pluto with a thickness of $c_4\ R/3 = 30$ km only, where R is Pluto's radius. Compact ices and amorphous silicates provide $h/s = 1.2$ and $c_5\rho_5 = 1720$ kg m^{-3}, which would make the bulk density of Pluto and Charon too inconsistent with a solar composition. The 67P h/s ratios match the value measured in 1P/Halley (Jessberger et al. 1989) and are much larger than $h/s = 0.2$ assumed so far in models of Pluto and Charon (McKinnon et al. 1997). Impacts, tidal stress and the decay of radionuclides may decrease the pristine ice content during KBO lifetimes, implying that the pristine KBO bulk density may increase in time, without in any way overcoming the upper limit $c_5\rho_5$.

5 CONCLUSIONS

For the first time, Rosetta data allowed us to constrain the dust-to-ices mass ratio in a Jupiter Family Comet by means of independent techniques. Also, thick dust deposits ubiquitous on 67P northern terrains allow us to infer that probably in all comets the dust-to-ices mass ratio inside the nucleus is about twice that most often measured in the lost material, e.g. by the RSI experiment and by trail observations. The water mass fraction of the dust deposits is $\approx 5\%$, very close to the water mass fraction sublimating from the average nucleus surface, thus making similar the activity from pristine terrains and that coming from the deposits. We obtain a pristine ice volume fraction of the 67P nucleus close to 20%, matching that directly provided by the bulk

density of Pluto, Charon and Triton, just assuming that the composition of their non-volatile material is that measured in comets (Fulle 2017). The possible highly variable content in carbon, and the ice volume fraction in comets and KBOs, lower than in CI-chondrites, suggest multiple scenarios of their formation. Icy objects in the protoplanetary disc may have formed everywhere outside the water snow-line, with a composition of non-volatiles apparently independent of the solar distance during accretion, thus confirming a fast mixing of non-volatiles in the protoplanetary disc (Ciesla 2011). This is further confirmed by the sub-mm aggregates of minerals of bulk density > 4000 kg m^{-3} observed by GIADA in 67P (Fig. 1). These minerals can have been formed only in the inner solar protoplanetary disc (Brownlee 2014). The variable ice content in KBOs suggests important migrations of the most icy objects (possibly comets and KBOs with a CI-chondritic composition of non-volatiles) outside the water snow-line, where they may have accreted. Memory of the accretion sun-distance may be preserved by the ratios D/H, O_2/H_2O and N_2/H_2O (Fulle et al. 2016b).

ACKNOWLEDGEMENTS

Rosetta is an ESA mission with contributions from its member states and NASA. Rosetta's Philae lander is provided by a consortium led by DLR, MPS, CNES and ASI. We thank all the Rosetta instrument teams, the Rosetta Science Ground Segment at ESAC, the Rosetta Mission Operations Centre at ESOC and the Rosetta Project at ESTEC for their outstanding work enabling the science return of the Rosetta Mission. GIADA was built by a consortium led by the Univ. Napoli Parthenope & INAF - Oss. Astr. Capodimonte, in collaboration with the Inst. de Astrofisica de Andalucia, ES, Selex-FI-IT and SENER-ES. GIADA is presently managed & operated by Ist. di Astrofisica e Planetologia Spaziali-INAF, IT. GIADA was funded and managed by the Agenzia Spaziale Italiana, IT, with the support of the Spanish Ministry of Education and Science MEC, ES. GIADA was developed from a PI proposal from the University of Kent; sci. & tech. contribution were provided by CISAS, IT, Lab. d'Astr. Spat., FR, and Institutions from UK, IT, FR, DE and USA. Science support was provided by NASA through the US Rosetta Project managed by the Jet Propulsion Laboratory/California Institute of Technology. We would like to thank Angioletta Coradini for her contribution as a GIADA Co-I. GIADA calibrated data will be available through ESA's PSA web site (www.rssd.esa.int/index.php?project=PSA&page=index). All data presented here are available on request prior to its archiving in the PSA. This research was supported by the Italian Space Agency (ASI) within the INAF-ASI agreements I/032/05/0 and I/024/12/0. SFG acknowledges the financial support of UK STFC (grant ST/L000776/1).

REFERENCES

Altwegg K. et al., 2015, Science 347, 1261952
Bertaux J. L., 2015, Astron. Astrophys. 583, A38
Blum J. et al., 2016, Mon. Not. Royal. Astr. Soc., this issue
Bockelée-Morvan D. et al., 2016, Mon. Not. Royal. Astr. Soc. 462, S170
Brownlee D., 2014, Ann. Rev. Earth Planet. Sci. 42, 179
Ciesla F. J., 2011, Astrophys. J. 740, 9
Della Corte V. et al., 2014, Journ. Astron. Instr. 3, 1, 1350011
Della Corte V. et al., 2015, Astron. Astrophys. 583, A13
Della Corte V., et al., 2016, Acta Astronautica 126, 205
Ferrari M., Della Corte V., Rotundi A., Rietmeijer F. J. M., 2014, Plan. Space Sci. 101, 53
Fougere N. et al., 2016, Mon. Not. Royal. Astr. Soc. 462, S156
Fray N., et al., 2016, Nature 538, 72
Fulle M., Levasseur-Regourd A.C., McBride N. & Hadamcik E., 2000, Astron. J. 119, 1968
Fulle M. et al., 2016a, Astrophys. J. 821, 19
Fulle M. et al., 2016b, Mon. Not. Royal. Astr. Soc. 462, S2
Fulle M. et al., 2016c, Mon. Not. Royal. Astr. Soc. 462, S132
Fulle M., 2017, Nature Astr. 1, 0018
Hansen K. et al., 2016, Mon. Not. Royal. Astr. Soc. 462, S491
Hartogh P. et al., 2011, Nature 478, 218
Jessberger E. K., Kissel J., Rahe J., 1989, in Origin and Evolution of Planetary and Satellite Atmospheres, Atreya S.K., Pollack J. B. & Matthews M. S. Eds., Tucson, University of Arizona Press, 167
Jorda A. et al., 2016, Icarus 277, 257
Keller H. U. et al., 2015a, Astron. Astrophys. 579, L5
Keller H. U. et al., 2015b, Astron. Astrophys. 583, A34
Kresak L., Kresakova M., 1987, in Symposium on the Diversity and Similarity of Comets, Rolfe E. J. & Battrick B. Eds., ESA SP-278, 739
Lodders K., 2003, Astrophys. J. 591, 1220
McKinnon W. B., Simonelli D. P., Schubert G., 1997, in Pluto and Charon, Stern S. A. & Tholen D. J. Eds., Tucson, University of Arizona Press, 295
Mottola S., et al., 2015, Science 349, aab0232
Newburn R. L., Spinrad H., 1985, Astron. J. 90, 2591
Pätzold M., et al., 2016, Am. Astron. Soc., DPS 48, 116.27
Robertson J., 2002, Materials Sci. & Engineering R37, 129
Rotundi A., et al., 2015, Science 347, aaa3905
Shinnaka Y., et al. 2017, Astron J. 153, 76
Sykes M. V., Walker R. G., 1992a, in Asteroids, Comets, Meteors, Lunar and Plan. Inst., 587
Sykes M. V., Walker R. G., 1992b, Icarus 95, 180

This paper has been typeset from a TEX/LATEX file prepared by the author.